



Published in final edited form as:

Cancer Discov. 2019 October ; 9(10): 1422–1437. doi:10.1158/2159-8290.CD-18-1259.

The mechanism of anti-PD-L1 antibody efficacy against PD-L1 negative tumors identifies NK cells expressing PD-L1 as a cytolytic effector

Wenjuan Dong^{1,2,#}, Xiaojin Wu^{3,4,#}, Shoubao Ma^{1,5,#}, Yufeng Wang^{3,#}, Ansel P. Nalin⁶, Zheng Zhu¹, Jianying Zhang⁷, Don M. Benson³, Kai He³, Michael A. Caligiuri^{1,2,8,9}, Jianhua Yu^{1,2,8,9}

¹Department of Hematology & Hematopoietic Cell Transplantation, City of Hope National Medical Center, Duarte, CA 91010

²Hematologic Malignancies and Stem Cell Transplantation Institute, City of Hope National Medical Center, Duarte, CA 91010

³The Ohio State University Comprehensive Cancer Center, Columbus, OH 43210

⁴Jiangsu Institute of Hematology, The First Affiliated Hospital of Soochow University, Suzhou, China

⁵Institute of Blood and Marrow Transplantation, Collaborative Innovation Center of Hematology, Soochow University, Suzhou 215006, China.

⁶Medical Scientist Training Program, The Ohio State University, Columbus, OH 43210

⁷Department of Computational and Quantitative Medicine, City of Hope National Medical Center, Duarte, CA 91010

⁸Department of Immuno-Oncology, Duarte, CA 91010

⁹City of Hope Comprehensive Cancer Center, Duarte, CA 91010

Abstract

Blockade of PD-L1 expression on tumor cells via anti-PD-L1 monoclonal antibody (mAb) has shown great promise for successful cancer treatment by overcoming T cell exhaustion; however,

Correspondences: Jianhua Yu, Ph.D., jjiayu@coh.org; Phone: (626)-218-6041; Michael A. Caligiuri, M.D., mcaligiuri@coh.org; Phone: (626) 218-4328; Address: 1500 E. Duarte Road, Duarte, KCRB, Bldg. 158, 3rd Floor, CA 91010.

#:These authors equally contribute to this study.

Authors' Contributions

Conception and design: W. Dong, Y. Wang, J. Yu

Development of methodology: W. Dong, X. Wu, S. Ma, Y. Wang, J. Yu

Acquisition of data (provided animals, acquired and managed patients, provided facilities, etc.): W. Dong, X. Wu, S. Ma, Z. Zhu, Y. Wang

Analysis and interpretation of data (e.g., statistical analysis, biostatistics, computational analysis): W. Dong, X. Wu, Z. Zhu, Y. Wang, A.P. Nalin, J. Zhang, K He.

Writing, review, and/or revision of the manuscript: W. Dong, S. Ma, A.P. Nalin, J. Yu, M. Caligiuri

Administrative, technical, or material support (i.e., reporting or organizing data, constructing databases): J. Zhang, D. Benson

Study supervision: J. Yu, M. Caligiuri

Funding Acquisition: J. Yu, M. Caligiuri

Disclosure of Potential Conflicts of Interest

Dr. Caligiuri is a shareholder of BeiGene. Other authors declare no conflict of interest.

the function of PD-L1 on NK cells and the effects of anti-PD-L1 mAb on PD-L1+ NK cells remain unknown. Moreover, patients with PD-L1⁻ tumors can respond favorably to anti-PD-L1 mAb therapy for unclear reasons. Here we show that some tumors can induce PD-L1 on NK cells via AKT signaling, resulting in enhanced NK cell function and preventing cell exhaustion. Anti-PD-L1 mAb directly acts on PD-L1+ NK cells against PD-L1⁻ tumors via a p38 pathway. Combination therapy of anti-PD-L1 mAb and NK cell-activating cytokines significantly improves therapeutic efficacy of human NK cells against PD-L1⁻ human leukemia when compared to monotherapy. Our discovery of a PD-1-independent mechanism of antitumor efficacy via the activation of PD-L1+ NK cells with anti-PD-L1 mAb offers new insights into NK cell activation and provides a potential explanation as to why some patients lacking PD-L1 expression on tumor cells still respond to anti-PD-L1 mAb therapy.

Keywords

PD-L1/PD-1; NF- κ B; atezolizumab; AML; NK cells

Introduction

Inhibition of the programmed death-1/programmed death ligand-1 (PD-1/PD-L1) pathway has become a very powerful therapeutic strategy for patients with cancer, and has shown unprecedented clinical responses in advanced liquid and solid tumors (1). At present, two PD-1 monoclonal antibodies (mAbs), pembrolizumab (Keytruda) and nivolumab (Opdivo), are FDA-approved to treat melanoma, kidney cancer, head and neck cancers, and Hodgkin's lymphoma (2–4). Three PD-L1 mAbs, atezolizumab (Tecentriq), avelumab (Bavencio), and durvalumab (Imfinzi), are FDA-approved to treat non-small cell lung cancer (NSCLC), bladder cancer, and Merkel cell carcinoma of the skin (5–7). However, the overall response rate to anti-PD-L1 mAb therapy is still very low in patients with melanoma (26%), NSCLC (21%), and renal cell carcinoma (13%) (8). In addition, anti-PD-L1 mAb therapy can also show an unexplained clinical response in the absence of PD-L1 expression on tumor cells (8,9). Therefore, an improved understanding of the mechanisms for anti-PD-L1 (or anti-PD-1) mAb therapy will help direct future efforts in developing more precise cancer immuno-therapeutics.

Tumor cells in the tumor microenvironment (TME) can upregulate PD-L1 after encountering activated T cells via their secretion of IFN- γ (10). Upon binding to PD-1, PD-L1 delivers a suppressive signal to T cells and an anti-apoptotic signal to tumor cells, leading to T cell dysfunction and tumor survival (10). Therefore, anti-PD-1/PD-L1 therapy aims to remove this immune suppression and activate the T cell response against cancer. It has been reported that PD-L1 is not only expressed on tumor cells but is also on immune cells including T cells, natural killer (NK) cells and macrophages within the TME (11–14). However, the function and the mechanism of action of PD-L1 on NK cells remain unexplored. It is also unknown as to whether and how anti-PD-L1 mAbs can modulate the function of NK cells expressing PD-L1. Unraveling these mechanisms will likely play an important role in the clinical effectiveness of anti-PD-1/PD-L1 mAb therapy.

NK cells comprise a group of innate cytolytic effector cells that participate in immune surveillance against cancer and viral infection. NK cells become cytolytic without prior activation especially when they encounter cells lacking self-MHC class I molecules (15). Downregulation of MHC class I can occur in the setting of cancer (16), allowing NK cells to recognize and lyse malignant cells. Activated NK cells exert strong cytotoxic effects via multiple mechanisms involving perforin, granzyme B, TRAIL, or FASL (17). NK cells also produce IFN- γ , which not only directly affects target cells, but also activates macrophages and T cells to kill tumor cells or enhance the antitumor activity of other immune cells (18). However, to our knowledge, the function of PD-L1 on NK cells and the underlying mechanisms in the normal or disease setting, as well as the involvement of PD-L1+ NK cells in anti-PD-L1 mAb therapy has not been explored.

In the present study, we found that some myeloid leukemic cell lines and acute myeloid leukemia (AML) blasts from patients can upregulate PD-L1 on NK cells. PD-L1+ NK cells are activated effectors exerting enhanced cytotoxic activity against target cells *in vitro* compared to PD-L1⁻ NK cells. NK cells from a majority of AML patients expressed moderate to high levels PD-L1 and the change in its level of expression following chemotherapy correlated with clinical response. Further, *in vivo*, anti-PD-L1 mAb treatment in combination with NK cell-activating cytokines significantly enhanced NK cell antitumor activity against myeloid leukemia lacking PD-L1 expression, suggesting that anti-PD-L1 mAb therapy has a unique therapeutic role in treating PD-L1⁻ cancer, acting through NK cells. This novel mechanism of direct innate immune cell activation with anti-PD-L1 mAb therapy that is PD-1-independent may explain the efficacy of the anti-PD-L1 checkpoint inhibitor in some PD-L1⁻ tumors.

RESULTS

PD-L1 expression on NK cells after encountering tumor cells

Expression of PD-L1 has been extensively reported on tumor cells and its binding to PD-1 on T cells suppresses the function of PD-1+ T cells (19). The expression of PD-L1 on immune cells has also been reported on macrophages, T cells and NK cells (11–14). However, the mechanism of induction and function of PD-L1 on NK cells remains unknown. Here, we enriched fresh human NK cells from healthy donors and co-cultured them with PD-L1^{10/-} target tumor cells, the K562 myeloid leukemia cell line. We found that anywhere from 14.2–74.4% of NK cells expressed PD-L1 after encountering K562 cells (Fig. 1A and Supplementary Fig. S1A). The RNA and protein levels for PD-L1 were both markedly increased (Fig. 1B and 1C). To confirm the expression of PD-L1 on NK cells, we stained both PD-L1⁻ and PD-L1+ NK cells with human NK cell surface marker CD56. Immunofluorescence images showed that PD-L1 (green) localized with CD56 (red) on PD-L1+ NK cells (Fig. 1D). In addition to its expression on the NK cell surface, PD-L1 can also be secreted by NK cells (Fig. 1E). To further understand the mechanism of K562-induced NK cell expression of PD-L1, we FACS-purified NK cells to repeat the experiments with highly enriched NK cells. We observed that PD-L1 was induced by specific interactions between K562 cells and purified NK cells (Fig. 1F). We also tested whether direct cell contact was required for PD-L1 induction. For this purpose, NK cells were cultured in the

supernatants from K562 cells alone or in the supernatants from K562 cells incubated with NK cells. The conditioned media marginally induced PD-L1, significantly less so when compared to NK cells directly incubated with K562 cells (Supplementary Fig. S1B). K562 cells incubated in transwells did not induce PD-L1 on NK cells (Fig. 1G). Of note, PD-L1 expression could also be more modestly induced on CD8⁺ T cells and B cells when co-incubated with K562 cells, but not in NK-T cells or CD4⁺ T cells (Supplementary Fig. S1C–G). Collectively, these results show that direct interaction between NK cells and K562 myeloid leukemia cells alone is sufficient to induce PD-L1 expression on NK cells.

PD-L1 expression marks NK cell activation and positively correlates with clinical outcome of AML patients

We next investigated the function of PD-L1 expression on NK cells. NK cell expression of CD107a and IFN- γ production are commonly used as functional markers for NK cell degranulation and cytokine production, respectively, following NK cell activation (17,20). While degranulation and IFN- γ production occurred within 2 h of NK cells encountering K562 cells (Supplementary Fig. S2A, top and middle panel), PD-L1 upregulation on NK cells increased significantly only after 16 h (Supplementary Fig. S2A, bottom panel). These data suggest that PD-L1 upregulation on NK cells is likely not the driver of NK cell activation but rather the result of NK cell activation. We compared the functional phenotype of PD-L1⁺ and PD-L1⁻ NK cells following co-culture with K562 cells. We found that the expression of CD107a and that of IFN- γ were significantly increased in PD-L1⁺ NK cells compared to PD-L1⁻ NK cells (Fig. 2A). The ⁵¹Cr release assay confirmed the cytotoxicity of PD-L1⁺ NK cells was dramatically increased compared to PD-L1⁻ NK cells (Fig. 2B). These results further suggest that PD-L1⁺ NK cells are highly activated immune effector cells. Giemsa staining showed that PD-L1⁺ NK cells were larger in size and had a thicker cytoplasm (Fig. 2C, top panel). The observation of the PD-L1⁺ NK cells appearing larger and functionally more activated than the PD-L1⁻ NK cells were confirmed by transmission electron microscopy (Fig. 2C, bottom panel). The cytoplasm of freshly isolated PD-L1⁺ NK cells contains more mitochondria and liposomes than the PD-L1⁻ NK cells, which may account for their larger size (Fig. 2C, bottom panel). We also examined the survival and proliferative capacity of PD-L1⁺ NK cells. Compared to PD-L1⁻ NK cells, PD-L1⁺ NK cells are more apoptotic (Fig. 2D–F). There was no difference in proliferation between PD-L1⁺ and PD-L1⁻ NK cells (Fig. 2G). Using flow cytometry, we measured the expression of surface markers present on these two NK cell subsets. We observed that the expression of the two activation antigens, CD69 and CD25, were significantly increased on PD-L1⁺ NK cells compared to PD-L1⁻ NK cells, while the receptors CD94, KLRG1, NKp44, NKG2D and TGF β R2 did not show a significant difference in expression between PD-L1⁺ and PD-L1⁻ NK cells (Supplementary Fig. S2B). CXCR4 expression was decreased on PD-L1⁺ NK cells compared to PD-L1⁻ NK cells, which could promote their egress from the bone marrow niche (21) (Supplementary Fig. S2B). These data demonstrate that PD-L1 can be induced in NK cells when encountering tumor cells and compared to PD-L1⁻ NK cells, PD-L1⁺ NK cells appear to possess higher levels of effector functions against tumor cells.

We next addressed whether PD-L1⁺ NK cells exist in cancer patients and whether this NK cell subset is correlated to clinical outcomes following standard chemotherapy. For this

purpose, we examined samples from 79 AML patients and found that the PD-L1+ NK cell population existed in the majority of AML patients but not in the healthy donors (Fig. 2H). The percentage of PD-L1+ NK cell population in the AML patients was as high as 40% with 77% (61/79) of the AML patients having PD-L1+ NK cells (Fig. 2H). We also confirmed the induction of PD-L1 on NK cells from healthy donors during *ex vivo* incubation with primary patient AML blasts (Fig. 2I and Supplementary Fig. S2C). When comparing the percentage of PD-L1+ NK cells in AML patients at the time of evaluation for response to two cycles of standard induction chemotherapy, we observed that AML patients who achieved complete remission (CR; n=31 of 47) had a significantly higher percentage of PD-L1+ NK cells at CR compared to the percentage of PD-L1+ NK cells at the time of diagnosis (Fig. 2J). In contrast, AML patients who did not achieve CR (NCR, n=16 of 47) showed no significant difference in percentage of PD-L1+ NK cells between the time of diagnosis and the time of assessment for CR (Fig. 2K). Further, AML patients who achieved CR had a significantly higher percentage of PD-L1+ NK cells compared to AML patients who did not achieve CR (Fig. 2L). When the data were reanalyzed and presented as the percent change of PD-L1+ NK cells from the time at diagnosis to the time of assessment for CR, a significant difference was also observed between the patients with CR and those without CR (Fig. 2M). However, these differences were not observed in the percentage of total NK cells at diagnosis when compared to the percentage of total NK cells at the time of CR evaluation, regardless of whether or not the AML patients achieved CR (Supplementary Fig. S2D–G). These data suggest that the percentage of PD-L1+ NK cells at the time of CR evaluation is correlated with attainment of CR, rather than the percentage of total NK cells. Taken together, the data presented thus far suggest that the activated NK cells as identified by their expression of PD-L1 may possess anti-leukemic activity *in vivo*.

Targeting PD-L1 with the humanized anti-PD-L1 mAb atezolizumab enhances NK cell function

We have found that PD-L1 expression or lack thereof could divide NK cells into two morphologically and functionally distinct populations with a higher level of cytotoxicity and IFN- γ production in the PD-L1+ subset compared to the PD-L1- subset. To further evaluate the function of PD-L1 on NK cells, we used atezolizumab (AZ, trade name Tecentriq), one of the humanized mAb against PD-L1 that has been approved by the Food and Drug Administration for the treatment of non-small cell lung cancer (NSCLC) (22). K562 myeloid leukemia cells express a low level of PD-L1 (Supplementary Fig. S3A), consistent with a previous report (23). To ensure no contribution from PD-L1 expression on K562 cells, we generated PD-L1 knockout (KO) K562 cells using the CRISPR-Cas9 system (Supplementary Fig. S3A). Lack of PD-L1 expression on K562 cells did not affect their ability to induce the expression of PD-L1 on NK cells (Supplementary Fig. S3B).

AZ is an IgG1 mAb engineered with a modification in the Fc domain that eliminates mAb-dependent cellular cytotoxicity (ADCC) (9). To ensure complete block of the potential ADCC effect in AZ-treated NK cells, we used a mAb that blocks the Fc receptor. We found that compared to AZ-treated PD-L1- NK cells, IgG-treated PD-L1+ NK cells, and IgG-treated PD-L1- NK cells, treatment of PD-L1+ NK cells with AZ significantly increased the expression of CD107a in an ADCC-independent fashion and resulted in enhanced leukemic

cell killing as measured by ^{51}Cr release assay (Fig. 3A and B). $\text{IFN-}\gamma$ is also increased in PD-L1+ NK cells (Fig. 3C). To further confirm our finding that PD-L1 positively regulates NK cell function, we undertook lentiviral transduction of PD-L1 into NK cells from healthy donors. The PD-L1-transduced NK cells showed a significant increase in their $\text{IFN-}\gamma$ production, compared to empty vector control-transduced NK cells (Fig. 3D), and this difference was further enhanced following treatment of the PD-L1-transduced NK cells with AZ (Fig. 3D). We also found that the expression of CD107a was significantly decreased in PD-L1 knockdown (KD) NK cells compared to the empty vector control group after encountering K562 cells in the presence of AZ (Supplementary Fig. S3C).

In addition, we found that PD-L1 expression of NK cells pretreated with K562 were further elevated at both the mRNA and protein levels in a time dependent manner after treatment with AZ (Fig. 3E and F), suggesting that PD-L1 signaling by AZ induces continuous upregulation of PD-L1, which then becomes available for additional activation by AZ.

Mouse PD-L1+ NK cells show enhanced antitumor activity *in vivo*

We next sought to test whether NK cells could be induced to express PD-L1 in the presence of tumor in an animal model, and whether PD-L1+ murine NK cells display similar functional activity as seen thus far with human NK cells *ex vivo*. We found that mouse NK cells constitutively express PD-L1, which is consistent with a previous report (24); however, we also found that its expression could be significantly increased in mice bearing the lymphoid tumor YAC-1 (Fig. 4A). For further *in vivo* functional study, we generated PD-L1 knockout YAC-1 cells (PD-L1 KO YAC-1) using the CRISPR-Cas9 system (Supplementary Fig. S4A). PD-L1+ NK cells in mice bearing PD-L1 KO YAC-1 tumors showed enhanced degranulation compared to PD-L1⁻ NK cells (Fig. 4B). To further study the function of PD-L1 on mouse NK cells, we used PD-L1^{-/-} mice and found that CD107a expression was significantly decreased on splenic NK cells in PD-L1^{-/-} mice and showed a similar trend in lungs compared to NK cells in WT mice engrafted with the PD-L1 KO YAC-1 tumor cells (Fig. 4C and D). *In vivo* anti-PD-L1 mAb treatment of mice bearing PD-L1 KO YAC-1 tumors increased CD107a expression on NK cells in WT mice but not on NK cells in PD-L1^{-/-} mice (Fig. 4C and D). In WT mice with PD-L1^{+/+} NK cells implanted with PD-L1 KO YAC-1 tumor cells, the tumor burden was significantly decreased when the anti-PD-L1 mAb was used compared to IgG control-treated mice (Fig. 4E and Supplementary Fig. S4B). This suggests that host cells' PD-L1 may play a positive role in controlling tumor development. However, for similar experiments with PD-L1^{-/-} mice (i.e., lack of PD-L1 expression on NK cells), we did not observe significant antitumor activity of anti-PD-L1 mAb vs. IgG control (Fig. 4E and Supplementary Fig. S4B). NK cell percentages did not change in tumor-bearing WT and PD-L1^{-/-} mice with or without PD-L1 mAb treatment (Supplementary Fig. S4C). We also observed that tumor burden was lower in WT mice compared to PD-L1^{-/-} mice, which led us to investigate whether the effect of anti-PD-L1 mAb was mediated by NK cells. We depleted NK cells in WT mice implanted with PD-L1 KO YAC-1 tumor cells and the mice were treated with an anti-PD-L1 mAb or IgG control (Supplementary Fig. S4D). We observed that when NK cells were absent, there were no significant antitumor effect of the anti-PD-L1 mAb (Fig. 4E and Supplementary Fig. S4B), suggesting that NK cells play a role in mediating the effects of anti-PD-L1 mAb in our

animal model. Together, these results suggest that PD-L1+ NK cells are essential for antitumor activity of the PD-L1 mAb in mice bearing PD-L1⁻ tumors, and that the antitumor effect of the mAb is acting directly on NK cells. Our *in vivo* mouse studies suggest that the use of anti-PD-L1 mAb to target PD-L1+ NK cells should be considered as a cancer immunotherapy for certain PD-L1⁻ tumors.

Anti-PD-L1 mAb augments human PD-L1⁺ NK cell antitumor activity *in vivo*

Having hypothesized from our AML patients' data that PD-L1+ NK cells could have antitumor activity *in vivo* (Fig. 2L and M), and having shown an improved antitumor effect of mouse NK cells by delivering an anti-PD-L1 mAb against a malignant mouse tumor lacking PD-L1 *in vivo*, we next attempted to reproduce this finding in an orthotopic mouse model using human NK cells and PD-L1 KO K562 myeloid leukemia followed by *in vivo* delivery of AZ versus placebo (placebo was PBS but not isotype IgG; to avoid NK-cell ADCC that is not active with AZ). For this purpose, we transplanted human primary NK cells into NSG mice, without or with PD-L1 KO K562 myeloid leukemia cells. We first showed that the presence of the PD-L1 KO K562 cells resulted in a very significant increase in the expression of PD-L1 on human NK cells *in vivo* (Fig. 5A). Treatment of these mice with either a placebo or the AZ resulted in the latter group showing a significant increase in NK cell expression of granzyme B, IFN- γ , and CD107a when compared to NK cells in the placebo-treated group (Fig. 5B). Further, we showed that the mice treated with AZ had a significantly lower tumor burden compared to the placebo-treated mice (Fig. 5C).

We next assessed the effects of NK cell-activating cytokines on NK cell PD-L1 expression in the absence or presence of K562 myeloid leukemia cells. Alone, IL-2 had essentially no effect on NK cell PD-L1 expression in the absence or presence of K562 cells (Supplementary Fig. S5A). In contrast, IL-12, -15 and -18 each had a moderate effect on NK cell PD-L1 expression in the absence or presence of the K562 cells, and this was further increased when used in various combinations as shown in Supplementary Fig. S5A. We further evaluated PD-L1 expression kinetics in culture with the strong stimuli IL-12 and IL-18, and found that PD-L1 expression on NK cells was similar to that seen with K562 cell co-incubation (Supplementary Fig. S5B). The IL-12 and IL-18 stimulated NK cells expressing PD-L1 showed markedly higher levels of cytotoxicity and IFN- γ production compared to PD-L1⁻ NK cells and untreated NK cells (Supplementary Fig. S5C and D). IFN- γ is a potent inducer of PD-L1 expression in tumor cells (25); however, blocking IFN- γ signaling did not affect NK cell PD-L1 expression induced by IL-12 and IL-18 despite this combination of cytokines inducing massive amounts of IFN- γ in NK cells (26) (Supplementary Fig. S5E). In addition, recombinant IFN- γ could not induce PD-L1 expression on NK cells alone or in combination with other cytokines (Supplementary Fig. S5F). We hypothesized that the cytokine-induced PD-L1 on NK cells should respond to AZ treatment, providing a rationale for exploring the combination of NK-activating cytokines and AZ for the treatment of cancer.

In an attempt to assess the effect of treatment with the humanized anti-PD-L1 mAb AZ on survival of mice engrafted with human NK cells and human PD-L1 KO K562 myeloid leukemia, we treated mice with various combinations of NK-activating cytokines in the

absence or presence of AZ. As predicted from our earlier *in vitro* work showing that IL-2 alone did not increase PD-L1 expression on NK cells (Supplementary Fig. S5A), the *in vivo* administration of IL-2 alone or its combination with AZ had minimal effect on survival and in both cases no mice survived longer than 16 days (Fig. 5D). The administration of combinations of IL-12 and IL-15 or IL-12 and IL-18 had substantial effects on increasing PD-L1 expression on NK cells *in vitro* (Supplementary Fig. S5A), but the combination of these three cytokines in the absence of AZ only modestly improved survival over IL-2 plus AZ, with no survival beyond day 21 (Fig. 5D). In contrast, mice treated with IL-12, IL-15 and IL-18 in combination with AZ, showed a significant improvement in survival with 50% of mice alive at day 40 (Fig. 5D). These data, together with Fig. 4E, suggesting that AZ directly acts on PD-L1+ human NK cells in the presence of three NK-activating cytokines to significantly prolong survival in mice engrafted with a lethal dose of human myeloid leukemia.

The PI3K/AKT signaling pathway regulates PD-L1 expression on NK cells

To investigate mechanisms by which PD-L1 is induced in NK cells by myeloid leukemia cells, we performed an RNA microarray to profile gene expression in PD-L1+ NK cells vs. PD-L1⁻ NK cells, both of which were FACS-purified from bulk NK cells after being co-cultured with K562 cells. The results showed that the PD-L1+ NK cell subset had higher expression levels of *TBX21* and *EOMES*, which are the two signature transcriptional factors required for NK cells to gain functional maturity (27,28). CD226 (DNAM-1), an activation marker for NK cells (29), had higher expression in PD-L1+ NK cells while the negative regulatory transcriptional factor, *SMAD3*, had lower expression levels in PD-L1+ NK cells (30) (Fig. 6A). These gene expression patterns indicate that PD-L1+ NK cells exert unique gene profiling compared to their PD-L1⁻ counterpart and are consistent with our above characterization showing that PD-L1+ NK cells are an activated NK cell subset. In addition, the microarray data implied that protein kinase B (AKT) signaling may be involved in regulating PD-L1 expression on NK cells (Fig. 6A). The AKT family contains three members AKT1, AKT2, and AKT3 (31). To test whether AKT signaling regulates PD-L1 expression on NK cells, we incubated them with K562 cells in the presence of a global AKT inhibitor against AKT1/2/3 (afuresertib), followed by measuring PD-L1 expression on NK cells. Treatment with afuresertib significantly reduced PD-L1 expression (Fig. 6B, top panel, and C), suggested that global AKT inhibition is capable of blocking PD-L1 expression. Upstream of the AKT cascade is phosphatidylinositol-3-kinase (PI3K). Treatment with the PI3K inhibitor wortmannin also significantly reduced PD-L1 expression on NK cells when incubated with K562 cells (Fig. 6B, middle panels, and Fig. 6C). We next sought to identify which transcription factor(s) downstream of PI3K/AKT signaling regulates PD-L1 expression in NK cells. We cloned a PD-L1 promoter 2.1 kb upstream of the transcription start site, co-transfected it with genes for specific transcription factors into 293T cells, and measured the activity of the PD-L1 promoter by luciferase assay. We found that most transcriptional factors of the PI3K/AKT cascade including XBP-1, FOXO-1, NFAT-2, and NFAT-4 did not activate the PD-L1 promoter (32–34); however, the PI3K/AKT downstream transcription factor p65 enhanced PD-L1 promoter activity 5-fold compared to empty vector control (Fig. 6D). The p65 subunit comprises part of the nuclear factor kappa B (NF- κ B) transcription complex, which plays a crucial role in inflammatory and immune responses

(35). We then confirmed the regulatory role of p65 in PD-L1 expression using a specific p65 inhibitor TPCK (Fig. 6B, bottom panel, and Fig. 6C). To validate the role of the PI3K/AKT/p65 pathway in regulating PD-L1 expression, we examined the binding of p65 with the *PD-L1* promoter. For this purpose, we co-transfected the PD-L1 promoter with AKT or p65 in 293T cells and observed that the introduced AKT or p65 led to the enhanced association of p65 with the *PD-L1* promoter compared to IgG control (Fig. 6E and F). These results collectively show that signaling through PI3K/AKT/NF- κ B plays a critical role in not only regulating NK cell activation, but also PD-L1 expression.

Since NK cell activation is usually triggered by recognizing the absence of MHC-I class molecules (15), we next wondered if tumor susceptibility to NK cell lysis is associated with NK cell induction of PD-L1 expression. For this purpose, we examined the expression of HLA-A, B, C on target cell lines and found that K562 and AML3 cells have significantly lower expression of HLA-A, B, C, and are highly susceptible to NK cell lysis and induce PD-L1 expression on NK cells (Supplementary Fig. S6A–C). In contrast, RPMI 8226, MOLM-13 and MV-4–11 cells have high levels of HLA-A, B, C, are not susceptible to NK cell lysis and could not efficiently activate NK cells or induce NK cell expression of PD-L1 (Supplementary Fig. S6A–C), even following an extended incubation time (Supplementary Fig. S6D). These data suggest that target susceptibility to NK cell cytotoxicity may be associated with the capacity of PD-L1 induction by tumor cells.

The above experiments reveal that tumor cells induce PD-L1 expression on NK cells via the PI3K/AKT/NF- κ B pathway (Fig. 6B and C). We also showed that the binding of AZ to tumor-induced PD-L1 on NK cells led to further NK cell activation (Fig. 3A and 3B), suggesting that the induced PD-L1 on NK cells may signal following treatment with AZ. We thus continued to explore the molecular mechanism(s) downstream of the PD-L1/AZ interaction in NK cells. For this purpose, we screened four kinases that have been reported downstream of PD-L1 signaling in other cells (36–38). Intracellular flow cytometry analysis in Supplementary Fig. S7 showed that the activity of p38, a kinase in regulating NK cell function and antitumor activity (39), was increased by AZ treatment, while the activities of p-ERK, p-AKT, or p-mTOR were not increased. These data were confirmed by immunoblotting of p38 and its downstream NF- κ B signaling family members, including p65 (RelA), RelB, and RelC (Fig. 6G and H). Interestingly, it was previously reported that PD-L1 signaling in PD-L1+ tumor cells is via the PI3K/AKT pathway (38); however, our data showed that PD-L1 signaling in PD-L1+ NK cells was not via the PI3K/AKT pathway in the presence of AZ (Supplementary Fig. S7A). The assays with the p38 inhibitors, SB203580 and SB202190, were found to reduce AZ-induced PD-L1 expression in the presence of PD-L1 KO K562 tumor cells, suggesting a positive regulatory effect of p38 signaling in this setting (Fig. 6I). Consistent with this, ChIP assay also showed that p38 signaling induced the binding of p65 to the *PD-L1* promoter (Fig. 6J). Functional assays demonstrated that the two p38 inhibitors, SB203580 and SB202190, also inhibited AZ-induced CD107a and IFN- γ expression of NK cells in the presence of PD-L1 KO K562 tumor cells (Fig. 6K).

Taken together, our data suggest a model involving PD-L1 upregulation on activated NK cells via the PI3K/AKT signaling pathway after NK cells and tumor cells encounter each other (Supplementary Fig. S8); the model also involves subsequent anti-PD-L1 mAb binding

to the upregulated PD-L1 on NK cells by tumor cells and further activation of NK cells via the p38 signaling; both events leading to NF- κ B activation, resulting in a positive feedback loop in the presence of excess AZ to continuously induce PD-L1 expression and to further activate NK cells. In the loop, the engagement of the anti-PD-L1 mAb with PD-L1 upregulates PD-L1 expression on the NK cell surface, providing more binding sites for anti-PD-L1 mAb that leads to continuous activation of p38, which further transduces a strong activation signaling to NK cells to maintain their cytotoxic and cytokine secretion features (Supplementary Fig. S8).

Discussion

It is well-known that PD-L1 is typically expressed on tumor cells, allowing them to suppress PD-1+ T cell function thereby enhancing the tumor's ability to evade the immune system (40). However, the functional consequences of PD-L1 expression on NK cells and the role of PD-L1+ NK cells in regulation of the immune response have not been characterized. In this study, we studied PD-L1+ and PD-L1⁻ NK cells in both humans and mice in the setting of PD-L1⁻ tumors. PD-L1+ NK cells were found to have significantly enhanced cytotoxicity and IFN- γ production compared to PD-L1⁻ NK cells. We show that NK cells, upon encountering and being activated by NK-susceptible tumor cells, not only secrete cytokine and cytolytic granules, but also upregulate PD-L1 on its surface via a PI3K/AKT/NF- κ B pathway. Upon engagement with the anti-PD-L1 mAb AZ, PD-L1 is able to further upregulate NK cell function through the p38 signaling pathway, thus serving as a functional activation antigen for NK cells. Using these *in vitro* observations, we employed a mouse model and an orthotopic mouse model of human NK cells and PD-L1⁻ K562 myeloid leukemia to show that in both models, anti-PD-L1 mAb acts directly on PD-L1+ NK cells to improve the antitumor activity of NK cell sensitive yet lethal tumors *in vivo*. Interestingly, in an attempt to find a correlation with human disease, we performed an analysis that provides preliminary evidence for a correlation between an increase in the percent of PD-L1+ NK cells from the time of diagnosis to the completion of induction chemotherapy, with the attainment of a CR. Collectively, the extensive experimental data presented here may provide an explanation as to why some patients lacking PD-L1 expression on tumor cells still respond to anti-PD-L1 mAb therapy (8,9). Further, when combined with our analysis of NK cell PD-L1 expression in 79 AML patients, one could speculate that the presence of PD-L1+ NK cells may identify certain patients whose tumors are more susceptible to NK cell lysis and may therefore benefit from a trial of anti-PD-L1 mAb without or with NK cell-activating cytokines, exploiting a novel pathway that is independent of T cells and PD-1.

T cells infiltrating into the TME are heterogeneous, containing both effector and bystander CD8+T cell populations (41,42). The higher percentage of effector T cells in the TME, the better the prognosis, and vice versa (43). However, there are fewer studies of NK cells within the TME, and little is known about PD-L1+ NK cells. We found that after encountering myeloid leukemia cells, a proportion of NK cells lost most of their cytotoxic activity and became "bystander like" with little or no expression of PD-L1; while a second fraction of NK cells emerged with strong induction of PD-L1 expression, a state of activation with enhanced effector function toward tumor target cells. We found that the more sensitive the target cell was to NK cytotoxicity (by virtue of its inverse correlation with

MHC Class I expression), and the more direct cell-cell contact of the NK cells with the target cells, the higher was the expression of PD-L1 and the stronger was the activation of the NK cell. As noted above, PD-L1 expression on patient NK cells may serve as an *in vivo* biomarker for patient tumors that are more likely to be susceptible to NK cell lysis.

We and others previously showed that PD-1 expression on NK cells results in a negative regulatory event upon engagement with its ligand (44–46) as is well known in T cells (40,47). Previous functional analysis indicates that compared to PD-1⁻ NK cells, PD-1⁺ NK cells are less activated with a lower level of degranulation and impaired cytokine production upon their interaction with tumor targets (46). In contrast, our current study showed that PD-L1⁺ NK cells are more activated compared to their PD-L1⁻ counterparts upon their interaction with tumor targets. We also showed that PD-L1 signaling via the p38/NF- κ B pathway is a positive regulatory event for NK cells upon PD-L1 engagement by anti-PD-L1 mAb, resulting in further expression of PD-L1 which, in the presence of excess anti-PD-L1 mAb further increased p38 signaling. This positive feedback loop continually provides intracellular signaling that allows the NK cell to retain an activated effector state (Supplementary Fig. S8). Both effects are very likely to contribute to the potent antitumor effect seen by NK cells in both the *in vitro* and *in vivo* modeling performed in this study. Importantly, we also discovered that the induction of PD-L1 expression following the NK cell interaction with a NK cell susceptible tumor cell target is via the PI3K/AKT/NF- κ B signaling pathway, distinct from the p38/NF- κ B signaling pathway that mediates the NK cell activation resulting from the interaction between NK cell PD-L1 and anti-PD-L1 mAb. However, we show that the simultaneous interaction of the PD-L1⁺ NK cell with both its tumor cell target and anti-PD-L1 mAb does result in an additive effect on NK cell activation, likely the result of both pathways ultimately driving increased activation of NF- κ B as shown in Supplementary Fig. S8.

Thus far, in immunotherapy, reversal and even enhancement of T cell antitumor activity through checkpoint blockade has had great success in the cancer clinic (48–50). It is therefore not unreasonable to believe that NK cell-based antitumor activity in the TME could also be reversed and enhanced. Here we show that anti-PD-L1 mAb therapy enhanced PD-L1⁺ NK cell function against PD-L1⁻ tumors in both mouse and human systems *in vitro* and significantly improved survival against a human PD-L1⁻ tumor in a PD-1-independent fashion *in vivo*. Further, in our *in vivo* mouse model, we demonstrated that the depletion of NK cells or using PD-L1^{-/-} mice significantly decreased the antitumor effect of anti-PD-L1 mAb therapy, suggesting that the antitumor effects are mediated directly by the NK cells following PD-L1 signaling within the TME. While our study could not exclude the possible role of other PD-L1⁺ immune cells including myeloid cells in PD-L1 antibody therapy, we documented the role of PD-L1⁺ NK cells in mediating the anti-tumor effect in this setting, revealing a new strategy for an increased and prolonged immune response of NK cells in the TME, likely applicable to some but not all tumors, and provides an explanation as to how immune therapy with anti-PD-L1 mAb can be effective in individuals whose tumors lack PD-L1 expression (8,9).

IL-12, IL-15 and IL-18 cytokines are known to activate and expand NK cells, and each has been investigated in clinical studies (51–54). IL-12 has demonstrated antitumor effects

through its regulation of both innate and adaptive immune cells (55). Recombinant human IL-15 has entered phase 1/2 clinical trials for various types of cancer (56). IL-15 has shown promising antitumor effects alone or in combination with other treatments (57,58). IL-18 also plays an important role in expansion and priming of NK cells (59,60). Our current study showed that the anti-PD-L1 mAb AZ had a significantly enhanced antitumor effect when administered in combination with these NK cell-activating cytokines, leading to a prolonged survival in mice engrafted with human NK cells and human myeloid leukemia, likely through the enhancement of NK cell function. Together with the clinical correlative data presented on 79 AML patients in this report, our *in vitro* and *in vivo* studies here suggest that for select AML patients with a significant fraction of PD-L1^{hi}/₊ NK cells at CR, an anti-PD-L1 mAb clinical trial at the time of CR could be considered in order to prevent disease relapse, ultimately in combination with an NK-activating cytokine such as IL-15. In addition to measuring NK cell function against autologous patient blasts pre- and post-anti-PD-L1 mAb administration *ex vivo*, one could get a preliminary indication of *in vivo* activity by assessing the time to relapse. This is particularly relevant when considering a highly vulnerable population such as elderly AML patients where the vast majority relapse within 2 years (61). It would also be interesting to determine if AML patients treated with anti-KIR mAb to block NK KIR interaction with MHC Class I had a higher expression of PD-L1 on their NK cells (62).

In summary, our study identified a novel and unique subset of NK cells characterized by surface expression of PD-L1 in a fraction of patients with AML, and we reproduced this finding with *both in vitro* and *in vivo* animal and human tumor modeling. We showed that binding of anti-PD-L1 mAb to PD-L1⁺ NK cells induced strong antitumor activity *in vitro* and *in vivo* and this process was independent of the PD-1/PD-L1 axis. These antitumor effects were shown to be dependent on both NK cells and their expression of PD-L1 and were effective against tumors lacking expression of PD-L1. Collectively, our experimental data suggest these PD-L1⁺ NK cells can be further activated *in vivo* for an additional antitumor effect, likely in combination with an NK-activating cytokine. PD-L1^{high}/₊ NK cells may identify a subset of AML patients whose tumors are more susceptible to NK cell lysis. We believe it may therefore be reasonable to consider anti-PD-L1 mAb therapy for the subset of AML patients with a fraction of PD-L1^{high}/₊ NK cells at CR, especially in the elderly where a substantial number of AML patients achieve CR but the vast majority relapse and die within 2 years (61). Finally, we believe that the data from this report can at least partly explain why some cancer patients with tumors lacking PD-L1 expression can respond favorably to anti-PD-L1 mAb checkpoint inhibitor therapy. PD-L1⁺ NK cells may prove to be another important immune effector cell for checkpoint inhibitor-based cancer immunotherapy.

Materials and methods

Patient samples

Peripheral blood samples from 48 healthy donors and 79 patients newly diagnosed with AML were recruited in this study between December 2017 and November 2018 at the First Affiliated Hospital of Soochow University, Suzhou, China. The diagnosis and classification

of AML patients were based on the revised French-American-British (FAB) classification and the 2008 World Health Organization (WHO) criteria (63,64). Then we followed 47 newly diagnosed patients for collection of PBMCs before and after treatment. The clinic characteristics of these 47 patients are listed in Supplementary Table 1. Among these 47 patients, 31 patients achieved CR, while 16 patients did not respond to the treatment. We compared the PD-L1 expression on the NK cells before and after the treatment among these patients. The patients received standard induction chemotherapy (idarubicin 10 mg/m²/day for 3 days, cytarabine 100 mg/m²/day for 7 days). We evaluated patients for CR after 2 cycles of standard induction chemotherapy. CR was defined by the following: bone marrow blasts less than 5%, absence of blasts with Auer rods, absence of extramedullary disease, absolute neutrophil count greater than $1.0 \times 10^9/L$, platelet count greater than $100 \times 10^9/L$, and independence of red cell transfusions. Patients who failed to achieve these hematologic parameters after 2 cycles of standard induction chemotherapy was considered to have chemo-resistant disease. The study protocol was approved by the institutional review board of the First Affiliated Hospital of Soochow University Ethics Committee. All patients gave written informed consent to their participation in the study, which followed the ethical guidelines of the Declaration of Helsinki.

Mice

NSG and BALB/c mice were purchased from the Jackson Laboratory and housed at the City of Hope animal facility. PD-L1^{-/-} mice were kindly provided by Dr. Defu Zeng, City of Hope Beckman Research Institute who originally received it from Dr. Lieping Chen (Yale University) and Dr. Haidong Dong (Mayo Clinic). All experiments were approved by the City of Hope Animal Care and Use Committee.

Cell lines

K562 and MV-4-11 were obtained from American Type Culture Collection (ATCC) within 6 months of this study. RPMI 8226, YAC-1, MOLM-13, and AML3 cells were obtained from the laboratory of M.A.C. These cells were cultured with Roswell Park Memorial Institute 1640 medium (RPMI 1640) supplied with 10% heat-inactivated fetal bovine serum (FBS, Sigma-Aldrich) and were grown in 37°C with 5% CO₂. No further authentication of these cell lines was performed. Cell morphology and growth characteristics were monitored during the study and compared with published reports to ensure their authenticity. All cell lines used in this study were determined to be negative for Mycoplasma prior to experiments using MycoAlert™ Mycoplasma Detection Kit (Lonza, Cat #. LT07-318). The latest test was on June 12, 2019. All cell lines were used within 10 passages after thawing.

Microarray

High quality total RNA isolated from FACS-sorted PD-L1⁺ and PD-L1⁻ NK cells were used for microarray analysis. The integrity and quantity of the RNA were checked by Agilent Bioanalyzer and Nanodrop RNA 6000, respectively. The Clariom™ D Assay chip was used for hybridization following the manufacturer's protocol. Gene expression profile was analyzed using transcriptome analysis console (TAC) 3.0 software. Data collected from three donors were used for microarray analysis.

Cytotoxicity assay

Cytotoxicity assays were performed as described previously (65). K562 target cells were labeled with ^{51}Cr for 1 h at 37°C . Cells were washed and co-incubated with effector cells (PD-L1⁺ and PD-L1⁻ NK cells) in a 96-well V-bottom plate at various effector to target (E/T) ratios for 4 h at 37°C . Following culture, supernatants were collected in a scintillation vial for analysis. The standard formula of $100 \times (\text{cpm}_{\text{experimental}} - \text{cpm}_{\text{spontaneous}}) / (\text{cpm}_{\text{maximal}} - \text{cpm}_{\text{spontaneous}})$ was used to calculate percentages of specific lysis, which were displayed as the mean of triplicate samples.

Statistical analysis

Two independent or paired groups were compared by Student's t-test or paired t-test. Multiple groups were compared using an ANOVA or linear mixed model for repeated measures. For survival data, Kaplan-Meier method was used to estimate survival functions and logrank test was applied to group comparisons. *P* values were corrected for multiple comparisons by Holm's method or the Holm-Sidak method. A *P* value less than 0.05 was considered statistically significant (* *P*<0.05; ** *P*<0.01, ***, *P*<0.001; ****, *P*<0.0001). For microarray data, paired t test with variance smoothing was applied to group comparisons for each gene after log base 2 transformation and noise-level gene filtering. Both fold change and mean number of false positives (i.e. 5 out of 10,000 genes) were used to identify the top genes.

Details Included in the Supplementary Methods and Materials

Cell culture; antibody staining and flow cytometry (flow antibodies used in this study were listed in Supplementary Table 2); immunostaining assay; immunoblotting assay; real-time PCR; ChIP assay; cytotoxicity assay; PD-L1-knockout cell line; mouse models; and data availability.

Supplementary Material

Refer to Web version on PubMed Central for supplementary material.

Acknowledgments

This work was supported by grants from the NIH (NS106170, AI129582, CA185301, CA068458, CA223400, and CA163205), the Leukemia & Lymphoma Society (6503-17 and 1364-19), the American Cancer Society Scholar Award (RSG-14-243-01-LIB), and the Gabrielle's Angel Cancer Research Foundation.

Financial support, including the source and number of grants, for each author:

Michael A. Caligiuri: NIH grants, CA068458, CA185301, CA163205 Jianhua Yu: NIH grants, AI129582, NS106170, CA223400, the Leukemia & Lymphoma Society (6503-17 and 1364-19), the American Cancer Society Scholar Award (RSG-14-243-01-LIB), and the Gabrielle's Angel Cancer Research Foundation (No. 87).

References

1. Chen L, Han X. Anti-PD-1/PD-L1 therapy of human cancer: past, present, and future. *J Clin Invest* 2015;125(9):3384-91 doi 10.1172/JCI80011. [PubMed: 26325035]

2. Rihawi K, Gelsomino F, Sperandi F, Melotti B, Fiorentino M, Casolari L, et al. Pembrolizumab in the treatment of metastatic non-small cell lung cancer: a review of current evidence. *Ther Adv Respir Dis* 2017;11(9):353–73 doi 10.1177/1753465817725486. [PubMed: 28818019]
3. Atkins MB, Plimack ER, Puzanov I, Fishman MN, McDermott DF, Cho DC, et al. Axitinib in combination with pembrolizumab in patients with advanced renal cell cancer: a non-randomised, open-label, dose-finding, and dose-expansion phase 1b trial. *Lancet Oncol* 2018;19(3):405–15 doi 10.1016/S1470-2045(18)30081-0. [PubMed: 29439857]
4. Ferris RL, Blumenschein G Jr., Fayette J, Guigay J, Colevas AD, Licitra L, et al. Nivolumab for Recurrent Squamous-Cell Carcinoma of the Head and Neck. *N Engl J Med* 2016;375(19):1856–67 doi 10.1056/NEJMoa1602252. [PubMed: 27718784]
5. Santini FC, Rudin CM. Atezolizumab for the treatment of non-small cell lung cancer. *Expert Rev Clin Pharmacol* 2017;10(9):935–45 doi 10.1080/17512433.2017.1356717. [PubMed: 28714780]
6. Kaufman HL, Russell J, Hamid O, Bhatia S, Terheyden P, D'Angelo SP, et al. Avelumab in patients with chemotherapy-refractory metastatic Merkel cell carcinoma: a multicentre, single-group, open-label, phase 2 trial. *Lancet Oncol* 2016;17(10):1374–85 doi 10.1016/S1470-2045(16)30364-3. [PubMed: 27592805]
7. Faiena I, Cummings AL, Crosetti AM, Pantuck AJ, Chamie K, Drakaki A. Durvalumab: an investigational anti-PD-L1 monoclonal antibody for the treatment of urothelial carcinoma. *Drug Des Devel Ther* 2018;12:209–15 doi 10.2147/DDDT.S141491.
8. Herbst RS, Soria JC, Kowanetz M, Fine GD, Hamid O, Gordon MS, et al. Predictive correlates of response to the anti-PD-L1 antibody MPDL3280A in cancer patients. *Nature* 2014;515(7528):563–7 doi 10.1038/nature14011. [PubMed: 25428504]
9. Powles T, Eder JP, Fine GD, Braiteh FS, Lortot Y, Cruz C, et al. MPDL3280A (anti-PD-L1) treatment leads to clinical activity in metastatic bladder cancer. *Nature* 2014;515(7528):558–62 doi 10.1038/nature13904. [PubMed: 25428503]
10. Mandai M, Hamanishi J, Abiko K, Matsumura N, Baba T, Konishi I. Dual Faces of IFN γ in Cancer Progression: A Role of PD-L1 Induction in the Determination of Pro- and Antitumor Immunity. *Clin Cancer Res* 2016;22(10):2329–34 doi 10.1158/1078-0432.CCR-16-0224. [PubMed: 27016309]
11. Hartley GP, Chow L, Ammons DT, Wheat WH, Dow SW. Programmed Cell Death Ligand 1 (PD-L1) Signaling Regulates Macrophage Proliferation and Activation. *Cancer Immunol Res* 2018;6(10):1260–73 doi 10.1158/2326-6066.CIR-17-0537. [PubMed: 30012633]
12. Iraolagoitia XL, Spallanzani RG, Torres NI, Araya RE, Ziblat A, Domaica CI, et al. NK Cells Restrain Spontaneous Antitumor CD8⁺ T Cell Priming through PD-1/PD-L1 Interactions with Dendritic Cells. *J Immunol* 2016;197(3):953–61 doi 10.4049/jimmunol.1502291. [PubMed: 27342842]
13. Latchman YE, Liang SC, Wu Y, Chernova T, Sobel RA, Klemm M, et al. PD-L1-deficient mice show that PD-L1 on T cells, antigen-presenting cells, and host tissues negatively regulates T cells. *Proc Natl Acad Sci U S A* 2004;101(29):10691–6 doi 10.1073/pnas.0307252101. [PubMed: 15249675]
14. Terme M, Ullrich E, Aymeric L, Meinhardt K, Coudert JD, Desbois M, et al. Cancer-induced immunosuppression: IL-18-elicited immunoablative NK cells. *Cancer Res* 2012;72(11):2757–67 doi 10.1158/0008-5472.CAN-11-3379. [PubMed: 22427351]
15. Lanier LL. NK cell recognition. *Annu Rev Immunol* 2005;23:225–74 doi 10.1146/annurev.immunol.23.021704.115526. [PubMed: 15771571]
16. Bubenik J Tumour MHC class I downregulation and immunotherapy (Review). *Oncol Rep* 2003;10(6):2005–8. [PubMed: 14534734]
17. Caligiuri MA. Human natural killer cells. *Blood* 2008;112(3):461–9 doi 10.1182/blood-2007-09-077438. [PubMed: 18650461]
18. Becknell B, Caligiuri MA. Natural killer cells in innate immunity and cancer. *J Immunother* 2008;31(8):685–92 doi 10.1097/CJI.0b013e318182de23. [PubMed: 18779751]
19. Pardoll DM. The blockade of immune checkpoints in cancer immunotherapy. *Nat Rev Cancer* 2012;12(4):252–64 doi 10.1038/nrc3239. [PubMed: 22437870]

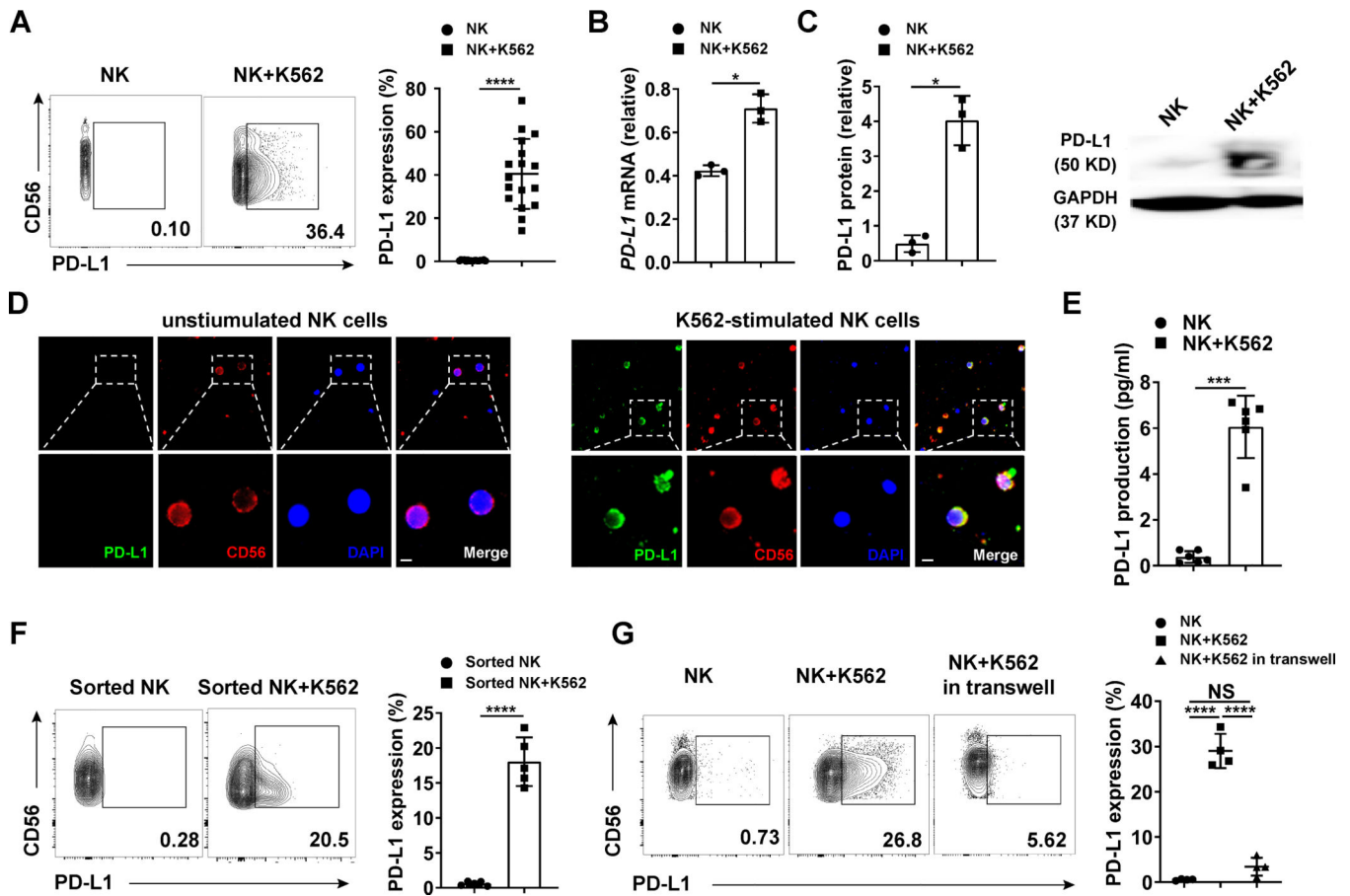
20. Alter G, Malenfant JM, Altfeld M. CD107a as a functional marker for the identification of natural killer cell activity. *J Immunol Methods* 2004;294(1–2):15–22 doi 10.1016/j.jim.2004.08.008. [PubMed: 15604012]
21. Beider K, Nagler A, Wald O, Frantza S, Dagan-Berger M, Wald H, et al. Involvement of CXCR4 and IL-2 in the homing and retention of human NK and NK T cells to the bone marrow and spleen of NOD/SCID mice. *Blood* 2003;102(6):1951–8 doi 10.1182/blood-2002-10-3293. [PubMed: 12730102]
22. Weinstock C, Khozin S, Suzman D, Zhang L, Tang S, Wahby S, et al. U.S. Food and Drug Administration Approval Summary: Atezolizumab for Metastatic Non–Small Cell Lung Cancer. *Clin Cancer Res* 2017;23(16):4534–9 doi 10.1158/1078-0432.ccr-17-0540. [PubMed: 28611199]
23. Berthon C, Driss V, Liu J, Kuranda K, Leleu X, Jouy N, et al. In acute myeloid leukemia, B7-H1 (PD-L1) protection of blasts from cytotoxic T cells is induced by TLR ligands and interferon-gamma and can be reversed using MEK inhibitors. *Cancer Immunol Immunother* 2010;59(12):1839–49 doi 10.1007/s00262-010-0909-y. [PubMed: 20814675]
24. Zhou J, Peng H, Li K, Qu K, Wang B, Wu Y, et al. Liver-Resident NK Cells Control Antiviral Activity of Hepatic T Cells via the PD-1-PD-L1 Axis. *Immunity* 2019;50(2):403–17 e4 doi 10.1016/j.immuni.2018.12.024. [PubMed: 30709740]
25. Blank C, Brown I, Peterson AC, Spiotto M, Iwai Y, Honjo T, et al. PD-L1/B7H-1 inhibits the effector phase of tumor rejection by T cell receptor (TCR) transgenic CD8+ T cells. *Cancer Res* 2004;64(3):1140–5. [PubMed: 14871849]
26. Yu J, Wei M, Becknell B, Trotta R, Liu S, Boyd Z, et al. Pro- and antiinflammatory cytokine signaling: reciprocal antagonism regulates interferon-gamma production by human natural killer cells. *Immunity* 2006;24(5):575–90 doi 10.1016/j.immuni.2006.03.016. [PubMed: 16713975]
27. Gordon SM, Chaix J, Rupp LJ, Wu J, Madera S, Sun JC, et al. The transcription factors T-bet and Eomes control key checkpoints of natural killer cell maturation. *Immunity* 2012;36(1):55–67 doi 10.1016/j.immuni.2011.11.016. [PubMed: 22261438]
28. Luetke-Eversloh M, Cicek BB, Siracusa F, Thom JT, Hamann A, Frischbutter S, et al. NK cells gain higher IFN-gamma competence during terminal differentiation. *Eur J Immunol* 2014;44(7):2074–84 doi 10.1002/eji.201344072. [PubMed: 24752800]
29. Zhang Z, Wu N, Lu Y, Davidson D, Colonna M, Veillette A. DNAM-1 controls NK cell activation via an ITT-like motif. *J Exp Med* 2015;212(12):2165–82 doi 10.1084/jem.20150792. [PubMed: 26552706]
30. Trotta R, Dal Col J, Yu J, Ciarlariello D, Thomas B, Zhang X, et al. TGF-beta utilizes SMAD3 to inhibit CD16-mediated IFN-gamma production and antibody-dependent cellular cytotoxicity in human NK cells. *J Immunol* 2008;181(6):3784–92. [PubMed: 18768831]
31. Martini M, De Santis MC, Braccini L, Gulluni F, Hirsch E. PI3K/AKT signaling pathway and cancer: an updated review. *Ann Med* 2014;46(6):372–83 doi 10.3109/07853890.2014.912836. [PubMed: 24897931]
32. Wang Y, Zhang Y, Yi P, Dong W, Nalin AP, Zhang J, et al. The IL-15-AKT-XBP1s signaling pathway contributes to effector functions and survival in human NK cells. *Nat Immunol* 2019;20(1):10–7 doi 10.1038/s41590-018-0265-1. [PubMed: 30538328]
33. Deng Y, Kerdiles Y, Chu J, Yuan S, Wang Y, Chen X, et al. Transcription factor Foxo1 is a negative regulator of natural killer cell maturation and function. *Immunity* 2015;42(3):457–70 doi 10.1016/j.immuni.2015.02.006. [PubMed: 25769609]
34. Mancini M, Toker A. NFAT proteins: emerging roles in cancer progression. *Nat Rev Cancer* 2009;9(11):810–20 doi 10.1038/nrc2735. [PubMed: 19851316]
35. Tak PP, Firestein GS. NF- κ B: a key role in inflammatory diseases. *J Clin Invest* 2001;107(1):7–11. [PubMed: 11134171]
36. Liu X, Wu X, Cao S, Harrington SM, Yin P, Mansfield AS, et al. B7-H1 antibodies lose antitumor activity due to activation of p38 MAPK that leads to apoptosis of tumor-reactive CD8(+) T cells. *Sci Rep* 2016;6:36722 doi 10.1038/srep36722. [PubMed: 27824138]
37. Gupta HB, Clark CA, Yuan B, Sareddy G, Pandeswara S, Padron AS, et al. Tumor cell-intrinsic PD-L1 promotes tumor-initiating cell generation and functions in melanoma and ovarian cancer. *Signal Transduct Target Ther* 2016;1 doi 10.1038/sigtrans.2016.30.

38. Dong P, Xiong Y, Yue J, Hanley SJB, Watari H. Tumor-Intrinsic PD-L1 Signaling in Cancer Initiation, Development and Treatment: Beyond Immune Evasion. *Front Oncol* 2018;8:386 doi 10.3389/fonc.2018.00386. [PubMed: 30283733]
39. Mavropoulos A, Sully G, Cope AP, Clark AR. Stabilization of IFN-gamma mRNA by MAPK p38 in IL-12- and IL-18-stimulated human NK cells. *Blood* 2005;105(1):282–8 doi 10.1182/blood-2004-07-2782. [PubMed: 15345584]
40. Kamphorst AO, Wieland A, Nasti T, Yang S, Zhang R, Barber DL, et al. Rescue of exhausted CD8 T cells by PD-1-targeted therapies is CD28-dependent. *Science* 2017;355(6332):1423–7 doi 10.1126/science.aaf0683. [PubMed: 28280249]
41. Simoni Y, Becht E, Fehlings M, Loh CY, Koo SL, Teng KWW, et al. Bystander CD8(+) T cells are abundant and phenotypically distinct in human tumour infiltrates. *Nature* 2018;557(7706):575–9 doi 10.1038/s41586-018-0130-2. [PubMed: 29769722]
42. Zheng C, Zheng L, Yoo JK, Guo H, Zhang Y, Guo X, et al. Landscape of Infiltrating T Cells in Liver Cancer Revealed by Single-Cell Sequencing. *Cell* 2017;169(7):1342–56 e16 doi 10.1016/j.cell.2017.05.035. [PubMed: 28622514]
43. Anderson KG, Stromnes IM, Greenberg PD. Obstacles Posed by the Tumor Microenvironment to T cell Activity: A Case for Synergistic Therapies. *Cancer Cell* 2017;31(3):311–25 doi 10.1016/j.ccell.2017.02.008. [PubMed: 28292435]
44. Liu Y, Cheng Y, Xu Y, Wang Z, Du X, Li C, et al. Increased expression of programmed cell death protein 1 on NK cells inhibits NK-cell-mediated anti-tumor function and indicates poor prognosis in digestive cancers. *Oncogene* 2017;36(44):6143–53 doi 10.1038/onc.2017.209. [PubMed: 28692048]
45. Benson DM Jr., Bakan CE, Mishra A, Hofmeister CC, Efebera Y, Becknell B, et al. The PD-1/PD-L1 axis modulates the natural killer cell versus multiple myeloma effect: a therapeutic target for CT-011, a novel monoclonal anti-PD-1 antibody. *Blood* 2010;116(13):2286–94 doi 10.1182/blood-2010-02-271874. [PubMed: 20460501]
46. Pesce S, Greppi M, Tabellini G, Rampinelli F, Parolini S, Olive D, et al. Identification of a subset of human natural killer cells expressing high levels of programmed death 1: A phenotypic and functional characterization. *J Allergy Clin Immunol* 2017;139(1):335–46 e3 doi 10.1016/j.jaci.2016.04.025. [PubMed: 27372564]
47. Hui E, Cheung J, Zhu J, Su X, Taylor MJ, Wallweber HA, et al. T cell costimulatory receptor CD28 is a primary target for PD-1-mediated inhibition. *Science* 2017;355(6332):1428–33 doi 10.1126/science.aaf1292. [PubMed: 28280247]
48. Sanmamed MF, Chen L. A Paradigm Shift in Cancer Immunotherapy: From Enhancement to Normalization. *Cell* 2018;175(2):313–26 doi 10.1016/j.cell.2018.09.035. [PubMed: 30290139]
49. Schwartzentruber DJ, Lawson DH, Richards JM, Conry RM, Miller DM, Treisman J, et al. gp100 peptide vaccine and interleukin-2 in patients with advanced melanoma. *N Engl J Med* 2011;364(22):2119–27 doi 10.1056/NEJMoa1012863. [PubMed: 21631324]
50. Ascierto PA, Del Vecchio M, Robert C, Mackiewicz A, Chiarion-Sileni V, Arance A, et al. Ipilimumab 10 mg/kg versus ipilimumab 3 mg/kg in patients with unresectable or metastatic melanoma: a randomised, double-blind, multicentre, phase 3 trial. *Lancet Oncol* 2017;18(5):611–22 doi 10.1016/S1470-2045(17)30231-0. [PubMed: 28359784]
51. Lenzi R, Edwards R, June C, Seiden MV, Garcia ME, Rosenblum M, et al. Phase II study of intraperitoneal recombinant interleukin-12 (rhIL-12) in patients with peritoneal carcinomatosis (residual disease < 1 cm) associated with ovarian cancer or primary peritoneal carcinoma. *J Transl Med* 2007;5:66 doi 10.1186/1479-5876-5-66. [PubMed: 18076766]
52. Gollob JA, Mier JW, Veenstra K, McDermott DF, Clancy D, Clancy M, et al. Phase I trial of twice-weekly intravenous interleukin 12 in patients with metastatic renal cell cancer or malignant melanoma: ability to maintain IFN-gamma induction is associated with clinical response. *Clin Cancer Res* 2000;6(5):1678–92. [PubMed: 10815886]
53. Conlon KC, Lugli E, Welles HC, Rosenberg SA, Fojo AT, Morris JC, et al. Redistribution, hyperproliferation, activation of natural killer cells and CD8 T cells, and cytokine production during first-in-human clinical trial of recombinant human interleukin-15 in patients with cancer. *J Clin Oncol* 2015;33(1):74–82 doi 10.1200/JCO.2014.57.3329. [PubMed: 25403209]

54. Robertson MJ, Stamatkin CW, Pelloso D, Weisenbach J, Prasad NK, Safa AR. A Dose-escalation Study of Recombinant Human Interleukin-18 in Combination With Ofatumumab After Autologous Peripheral Blood Stem Cell Transplantation for Lymphoma. *J Immunother* 2018;41(3):151–7 doi 10.1097/CJI.000000000000220. [PubMed: 29517616]
55. Tugues S, Burkhard SH, Ohs I, Vrohings M, Nussbaum K, Vom Berg J, et al. New insights into IL-12-mediated tumor suppression. *Cell Death Differ* 2015;22(2):237–46 doi 10.1038/cdd.2014.134. [PubMed: 25190142]
56. Perez-Martinez A, Fernandez L, Valentin J, Martinez-Romera I, Corral MD, Ramirez M, et al. A phase I/II trial of interleukin-15--stimulated natural killer cell infusion after haplo-identical stem cell transplantation for pediatric refractory solid tumors. *Cytotherapy* 2015;17(11):1594–603 doi 10.1016/j.jeyt.2015.07.011. [PubMed: 26341478]
57. Yan Y, Li S, Jia T, Du X, Xu Y, Zhao Y, et al. Combined therapy with CTL cells and oncolytic adenovirus expressing IL-15-induced enhanced antitumor activity. *Tumour Biol* 2015;36(6):4535–43 doi 10.1007/s13277-015-3098-7. [PubMed: 25627006]
58. Sim GC, Radvanyi L. The IL-2 cytokine family in cancer immunotherapy. *Cytokine Growth Factor Rev* 2014;25(4):377–90 doi 10.1016/j.cytogfr.2014.07.018. [PubMed: 25200249]
59. Madera S, Sun JC. Cutting edge: stage-specific requirement of IL-18 for antiviral NK cell expansion. *J Immunol* 2015;194(4):1408–12 doi 10.4049/jimmunol.1402001. [PubMed: 25589075]
60. Chaix J, Tessmer MS, Hoebe K, Fuseri N, Ryffel B, Dalod M, et al. Cutting edge: Priming of NK cells by IL-18. *J Immunol* 2008;181(3):1627–31. [PubMed: 18641298]
61. Kolitz JE. Very late relapse of acute myeloid leukemia. *Leuk Lymphoma* 2007;48(1):3–4 doi 10.1080/10428190601074497. [PubMed: 17325840]
62. Vey N, Dumas P-Y, Recher C, Gastaud L, Lioure B, Bulabois C- E, et al. Randomized phase 2 trial of lirilumab (anti-KIR monoclonal antibody, mAb) as maintenance treatment in elderly patients (pts) with acute myeloid leukemia (AML): results of the Effikir trial. Volume 130 Am Soc Hematology; 2017 p 889.
63. Bennett JM, Catovsky D, Daniel MT, Flandrin G, Galton DA, Gralnick HR, et al. Proposed revised criteria for the classification of acute myeloid leukemia. A report of the French-American-British Cooperative Group. *Ann Intern Med* 1985;103(4):620–5. [PubMed: 3862359]
64. Vardiman JW, Thiele J, Arber DA, Brunning RD, Borowitz MJ, Porwit A, et al. The 2008 revision of the World Health Organization (WHO) classification of myeloid neoplasms and acute leukemia: rationale and important changes. *Blood* 2009;114(5):937–51 doi 10.1182/blood-2009-03-209262. [PubMed: 19357394]
65. Yu J, Wei M, Becknell B, Trotta R, Liu S, Boyd Z, et al. Pro- and Antiinflammatory Cytokine Signaling: Reciprocal Antagonism Regulates Interferon-gamma Production by Human Natural Killer Cells. *Immunity* 2006;24(5):575–90 doi 10.1016/j.immuni.2006.03.016. [PubMed: 16713975]
66. Denman CJ, Senyukov VV, Somanchi SS, Phatarpekar PV, Kopp LM, Johnson JL, et al. Membrane-bound IL-21 promotes sustained ex vivo proliferation of human natural killer cells. *PLoS One* 2012;7(1):e30264 doi 10.1371/journal.pone.0030264.

SIGNIFICANCE

Targeting PD-L1 expressed on PD-L1+ tumors with anti-PD-L1 mAb successfully overcomes T-cell exhaustion to control cancer, yet patients with PD-L1⁻ tumors can respond to anti-PD-L1 mAb. Here we show that anti-PD-L1 mAb activates PD-L1+ NK cells to control growth of PD-L1⁻ tumors *in vivo*, and does so independent of PD-1.

**Fig. 1.**

Expression of PD-L1 on NK cells incubated with K562 myeloid leukemia cells for 24 h in the presence of IL-2. (A) Representative flow cytometry plots and summary data ($n = 17$) showing PD-L1 expression on enriched healthy donor-derived NK cells incubated without or with K562 cells in the presence of IL-2 (10 ng/ml, same for all panels). IL-2 was required to sustain NK cell survival *ex vivo* but alone had no effect on NK cell PD-L1 expression. (B) NK cells were incubated without or with K562 cells, and relative *PD-L1* mRNA expression was measured by qRT-PCR. The experiment was repeated three times. (C) Summary immunoblot data ($n = 3$) and representative example showing total PD-L1 protein in NK cells incubated without or with K562 cells. Total PD-L1 protein was measured by immunoblot and the relative expression rate was calculated by Image J. (D) Immunofluorescence of unstimulated (Left) and K562 cell-stimulated (Right) enriched human NK cells were stained with PD-L1 (green), CD56 (red) or DAPI nuclear stain (blue) and then merged. Images are shown at $20\times$ magnification (scale bar, $5\ \mu\text{m}$; top panels). Panels at the bottom are zoomed areas of dashed boxes in the top panels. (E) NK cells were incubated without or with K562, followed by measuring secreted PD-L1 protein levels by ELISA ($n = 6$). (F) Representative flow cytometry plots and summary data ($n = 5$) of FACS-purified NK cells (purity $> 96\%$) incubated with or without K562 cells. PD-L1 expression was measured by flow cytometry. (G) Representative flow cytometry plots and summary data ($n = 4$) showing the percentages of PD-L1+ NK cells from enriched NK cells incubated

with or without K562 cells in transwell plates, or incubated directly with or without K562 cells. Paired t test (A to F) was used for two-group comparisons and one-way ANOVA with repeated measures for donor-matched 3 groups (G). *P* values were adjusted by the Holm-Sidak method. NS, not significant. *, *P* < 0.05; ***, *P* < 0.001; ****, *P* < 0.0001.

Author Manuscript

Author Manuscript

Author Manuscript

Author Manuscript

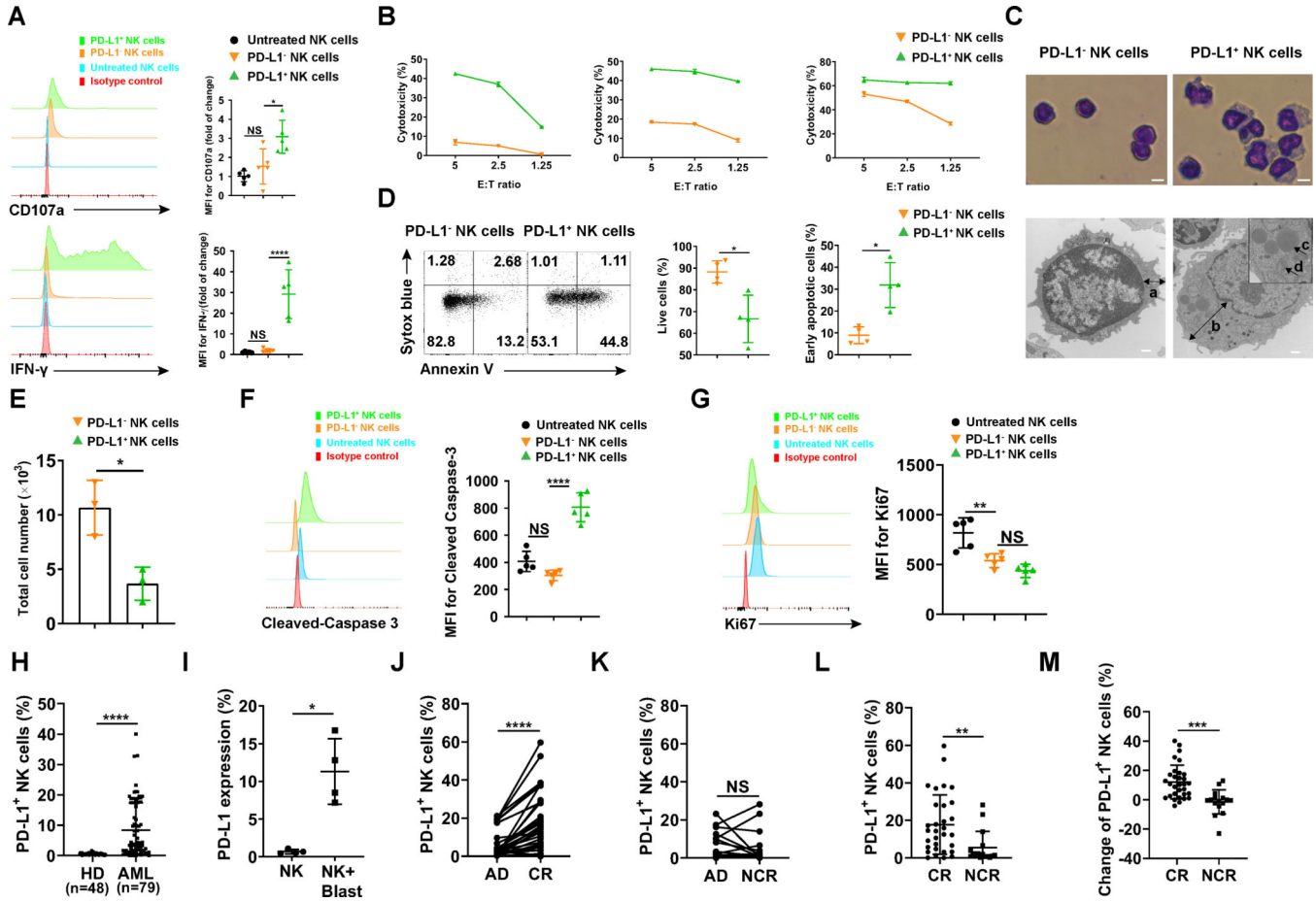


Fig. 2. Functionality assessment of the PD-L1+ NK cell subset. (A) Representative flow cytometry plots and summary data (n = 5) showing the expression of CD107a and IFN- γ in PD-L1⁻ and PD-L1⁺ NK cells induced by K562 myeloid leukemia cells for 24 h in the presence of 10 ng/ml IL-2. (B) PD-L1⁻ and PD-L1⁺ NK cells described in A were sorted to > 96% purity to measure cytotoxicity against K562 target cells by standard ⁵¹Cr release assay (n = 3). (C) Top panel: Giemsa staining of FACS-purified PD-L1⁻ and PD-L1⁺ NK cells. Representative images are shown at 20 \times magnification (scale bar, 5 μ m). Bottom panel: Transmission electron microscopy images of PD-L1⁻ and PD-L1⁺ NK cells. Left images: 17,000 \times magnification. Right image: 11,500 \times magnification (scale bar, 500 nm) with further magnification in the squared area. Arrows a and b: thickness of cytoplasm; Arrow c: liposome; Arrow d: mitochondria. (D) Representative flow cytometry plots and summary data (n = 4) of NK cells incubated with K562 cells for 72 h in the presence of IL-2. Live and early apoptotic PD-L1⁻ and PD-L1⁺ NK cells were measured by Sytox blue and Annexin V staining. (E) PD-L1⁻ and PD-L1⁺ NK cells were FACS-purified and incubated with feeder cells [feeder cells were K562 cells with membrane-bound IL-21 (66), treated with 100 Gy radiation] in the presence of IL-2 (n = 3). Feeder cells were added to NK cells at a ratio of 1:1 on days 1, 7, and 14. Live NK cells were counted by trypan blue exclusion at day 20 when all feeder cells were dead. (F) Representative flow cytometry plots and summary data (n = 5) of cleaved-Caspase 3 and (G) Ki67 in PD-L1⁻ and PD-L1⁺ NK cells. (H) PD-L1⁺ NK cells (%) in HD (n=48) and AML (n=79) patients. (I) PD-L1 expression (%) in NK and NK+ Blast. (J) PD-L1⁺ NK cells (%) in AD and CR. (K) PD-L1⁺ NK cells (%) in AD and NCR. (L) PD-L1⁺ NK cells (%) in CR and NCR. (M) Change of PD-L1⁺ NK cells (%) between CR and NCR.

Percentages of PD-L1+ NK cells in the peripheral blood of 48 healthy donors and 79 patients with AML at time of initial diagnosis. (I) PD-L1 expression on NK cells from healthy donors incubated with primary patient AML blasts (n = 4 AML patients). (J) Percentages of PD-L1+ NK cells at time of diagnosis and at time of evaluation for response following standard induction chemotherapy in AML patients who achieved a CR (n = paired groups of 31) and (K) those who did not achieve a CR (NCR, n = paired groups of 16). (L) Percentages of PD-L1+ NK cells at time of evaluation for response in AML patients who did (CR) and did not (NCR) achieve a CR following standard induction chemotherapy. (M) Percentage change of PD-L1+ NK cells (calculated by comparing PD-L1+ NK cells at diagnosis and at time of evaluation for response) in patients who achieve a CR and those who did not achieve a CR (NCR). Paired t test (D-E and H-M) was used for two-group comparisons and one-way ANOVA with repeated measures for donor-matched 3 groups (A, F and G). *P* values were adjusted by the Holm-Sidak method. *, *P* < 0.05; **, *P* < 0.01; ***, *P* < 0.001; ****, *P* < 0.0001; NS, not significant. HD, healthy donor; AD, after diagnosis; CR, complete response; NCR, no complete response. MFI, mean fluorescence intensity.

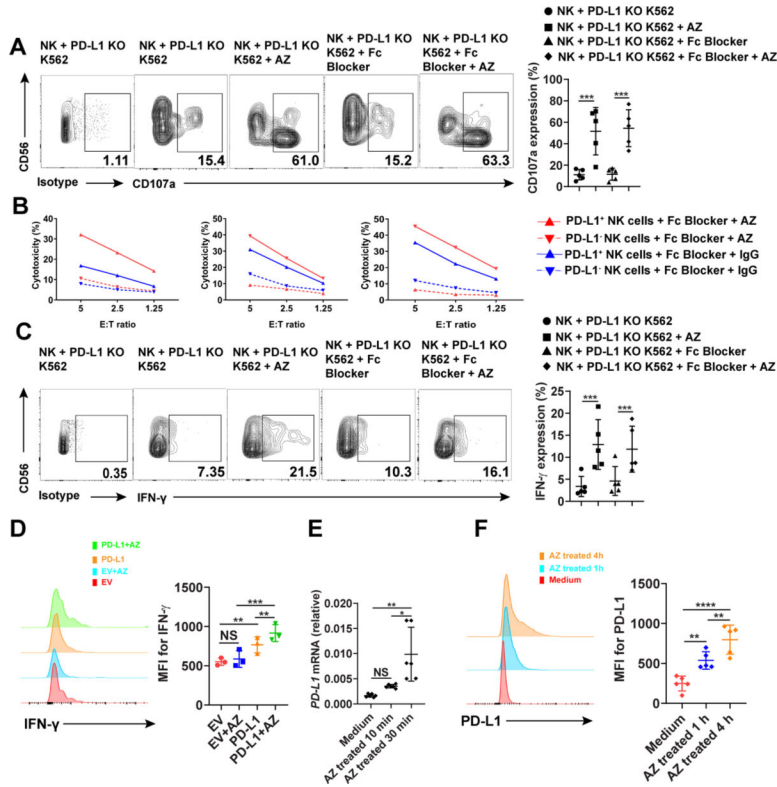


Fig. 3. Analysis of PD-L1 signaling and functions in NK cells upon anti-PD-L1 mAb AZ treatment. (A) NK cells were incubated with K562 cells for 24 h and then treated with or without 20 $\mu\text{g/ml}$ AZ in the presence or absence of an Fc blocker for 4 h. PD-L1+ NK cells were gated to assess the expression of CD107a ($n = 5$). AZ-treated cells were stained with anti-AZ antibody and non-AZ treated cells were stained with anti-PD-L1 antibody. (B) NK cells were incubated with K562 cells for 24 h and then treated with 20 $\mu\text{g/ml}$ AZ or IgG control in the presence of an Fc blocker for 4 h. AZ-treated PD-L1⁻ NK cells, AZ-treated PD-L1⁺ NK cells, IgG-treated PD-L1⁻ NK cells and IgG-treated PD-L1⁺ NK cells were sorted to >96% purity to measure cytotoxicity against K562 target cells by standard ⁵¹Cr release assay ($n = 3$). (C) Experiment in (A) were repeated to measure IFN- γ expression by intracellular flow cytometry. (D) Representative flow cytometry plots and summary data ($n = 3$) of NK cells transduced with empty vector (EV) or PD-L1 overexpression vector with or without AZ treatment prior to measuring the expression of IFN- γ by intracellular flow cytometry ($n = 3$). (E) Enriched NK cells were incubated with PD-L1 KO K562 cells for 20 h and then treated with 20 $\mu\text{g/ml}$ AZ for the indicated time on the x axis. NK cells were then sorted to > 96% purity and the relative levels of *PD-L1* mRNA expression were measured by qRT-PCR ($n = 6$). (F) Representative flow cytometry plots and summary data ($n = 5$) showing that the expression of PD-L1 on NK cells increases in a time dependent manner after treatment with AZ. One-way ANOVA with repeated measures (D-F) or linear mixed model (A and C) was used to compare donor-matched 3 or more groups. *P* values were adjusted by the Holm-Sidak method. *, $P < 0.05$; **, $P < 0.01$; ***, $P < 0.001$; ****, $P < 0.0001$; NS, not significant.

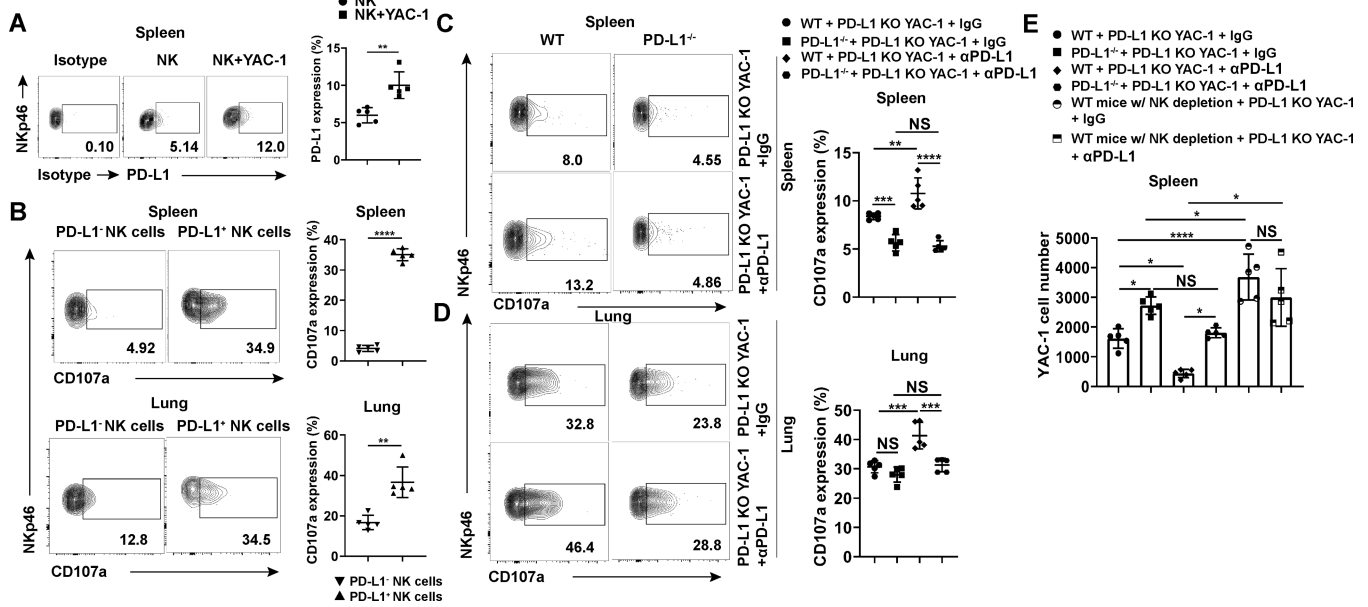


Fig. 4. PD-L1 KO mice and NK cell depletion show impaired antitumor activity in a PD-L1 knock-out YAC-1 tumor model treated with or without anti-PD-L1 mAb. (A and B) Representative flow cytometry plots and summary data (n = 5) of (A) PD-L1 expression of spleen NK cells and (B) CD107a expression of spleen and lung NK cells of BALB/c mice after being challenged with PD-L1 KO YAC-1 cells. (C and D) Representative flow cytometry plots and summary data (n = 5) of NK cell CD107a expression in the (C) spleen and (D) lung of WT and PD-L1^{-/-} BALB/c mice challenged with PD-L1 KO YAC-1 cells treated without or with anti-PD-L1 mAb. (E) The number of PD-L1 KO YAC-1 cells in spleens of WT, NK cell-depleted or PD-L1^{-/-} BALB/c mice (n = 5) treated with anti-PD-L1 mAb or IgG control. Paired t test (B and C) was used for two-group comparisons and one-way ANOVA with repeated measures for 3 or more groups (A and E). *P* values were adjusted by the Holm-Sidak method. *, *P* < 0.05; **, *P* < 0.01; ***, *P* < 0.001; ****, *P* < 0.0001.

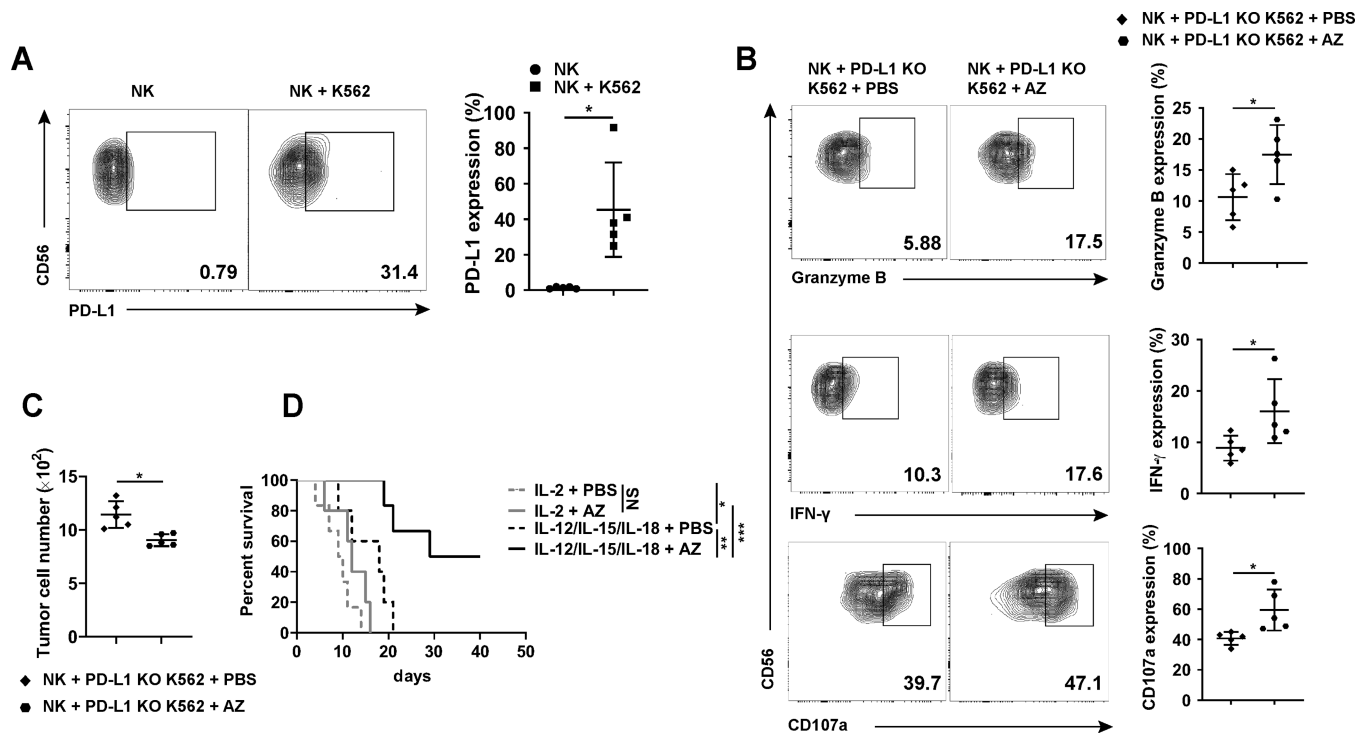


Fig. 5. Effects of the anti-PD-L1 mAb AZ and/or NK-activating cytokines on antitumor efficacy in vivo. (A) Human NK cells were injected i.v. into NSG mice without or with PD-L1 KO K562 cells followed by i.p. injection of 1 μ g IL-12 and 1 μ g IL-15 per mouse every other day. After 6 days, mice were sacrificed, and NK cells were isolated and assessed for PD-L1 expression by flow cytometry. Representative flow cytometric analyses and summary data are shown (n = 5). (B and C) Human NK cells and PD-L1 KO K562 cells were injected i.v. into NSG mice, followed by treatment with i.p. injection of AZ or PBS every other day. PBS was used instead of IgG1 as placebo because AZ lacks antibody-dependent cellular cytotoxicity activity. After 6 days (three treatments), mice were sacrificed and human NK cells were examined for (B) their expression of granzyme B, CD107a, and IFN- γ or (C) the number of PD-L1 KO K562 cells by flow cytometry. Representative analyses and summary data (n = 5) are shown. (D) Survival curve of NSG mice injected i.v. with primary human NK cells and PD-L1 KO K562 cells followed by treatment with IL-2 plus PBS, or IL-2 plus AZ, or the combination of IL-12, IL-15 and IL-18 plus PBS, or the combination of IL-12, IL-15 and IL-18 plus AZ every other day for two weeks. Two paired groups were compared by paired t test (A-C). Kaplan-Meier method was used to estimate survival functions and log rank test was applied to group comparisons (D). *, $P < 0.05$; **, $P < 0.01$; ***, $P < 0.001$; NS, not significant.

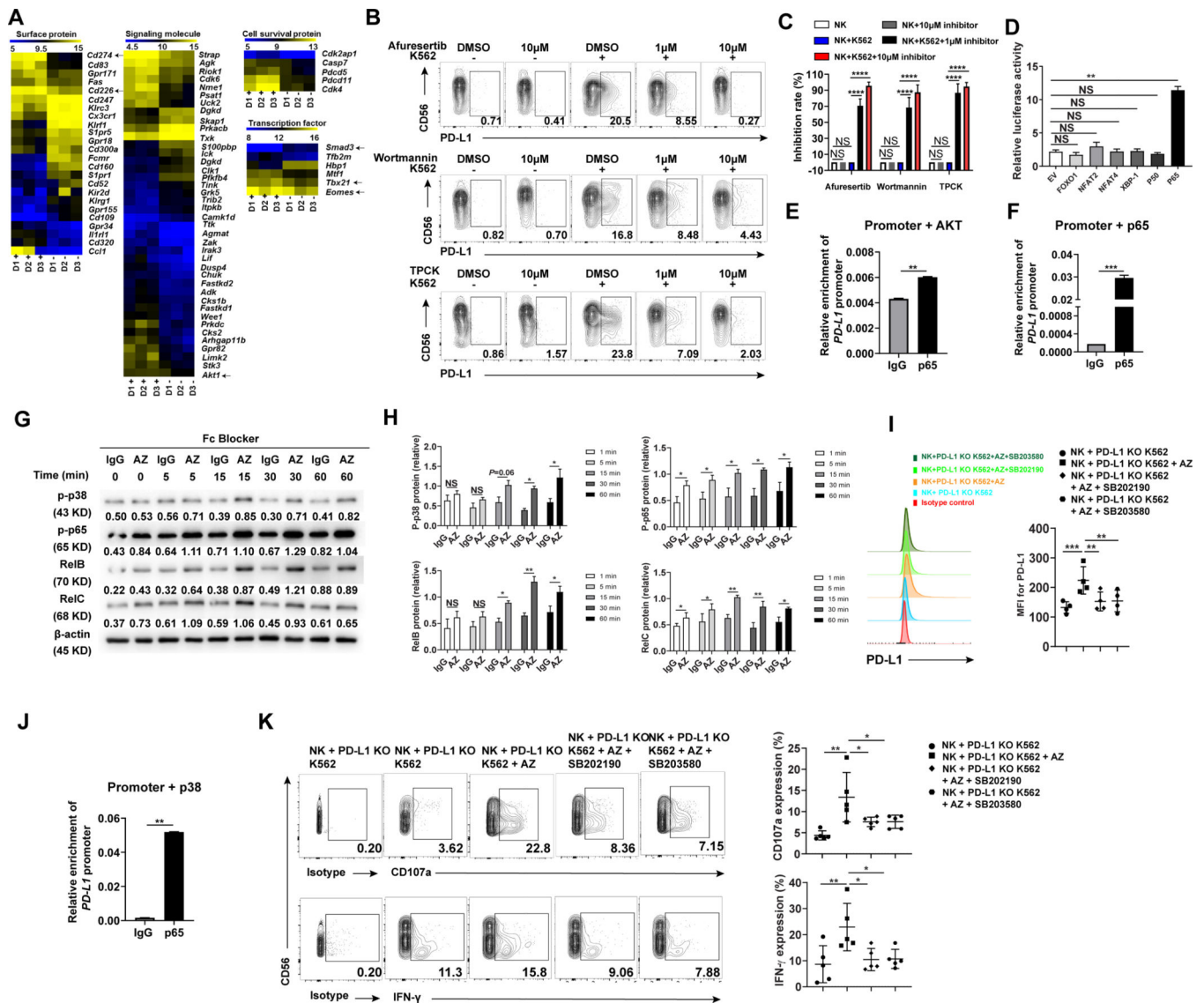


Fig. 6. Signaling pathways involved in the anti-PD-L1 antibody-induced NK cell activation in the presence of tumor cells. (A) Gene expression profile using RNA microarray of PD-L1⁻ and PD-L1⁺ NK cells sorted from K562 and IL-2-stimulated enriched NK cells of three healthy donors (D1, D2 and D3). “D1+” represents PD-L1⁺ NK cells from donor 1, while “D1-” represents PD-L1⁻ NK cells from donor 1, each purified by FACS sorting. Similar definitions are applied to “D2+”, “D2-”, “D3+”, and “D3-”. Expression of *Cd274* (PD-L1), *Cd226* (*DNAM-1*), *Tbx21*, *Eomes*, *Smad3*, and *Akt1* were highlighted by black arrows. (B) NK cells were incubated without or with K562 cells in the absence or presence of the AKT-pan inhibitor Afureserlib, the PI3K-specific inhibitor wortmannin or the P65-specific inhibitor TPCK at a concentration of 1 μM or 10 μM. The percentages of PD-L1⁺ NK cells were measured by flow cytometry. (C) Inhibition rate of PD-L1⁺ NK cells was measured as the relative proportion of PD-L1⁺ cells in each treatment condition compared to untreated control (no inhibition) (n = 5). (D) 293 T cells were transfected with the *PD-L1* promoter

and the indicated expression plasmids. Relative promoter activity was measured by luciferase assay after 48 h. (E and F) The chromatin immunoprecipitation (ChIP) assay was employed to assess the binding of p65 to the *PD-L1* promoter when (E) AKT or (F) p65 was overexpressed. The experiments were repeated three times. (G and H) Representative and summary data (n = 3) showing the activity of p38 and NF- κ B family members including p65 (RelA), RelB, and RelC in NK cells incubated with IL-2 plus PD-L1 KO K562 cells for 20 h and then with the anti-PD-L1 mAb AZ or IgG for various periods as indicated. Fc blocker was added 15 min prior to adding IgG or AZ antibodies to minimize ADCC effect. Total PD-L1 protein was measured by immunoblotting. Numbers beneath each lane represents relative density quantified by Image J software, normalized for equivalent loading as determined by β -actin. Increased phosphorylation of some members by AZ at 0 min likely due to the activation of the cells by AZ during sample harvesting. Linear mixed model was used to assess the treatment \times time interaction and group difference IgG vs AZ at each time point by accounting for the repeated measures from the same donor. (I) Flow cytometry to measure PD-L1 expression on NK cells incubated with PD-L1 KO K562 cells for 20 h and then with the anti-PD-L1 mAb AZ in the absence or presence of 1 μ M p38 inhibitor SB202190 or SB203580 for 4 h (n = 4). (J) The chromatin immunoprecipitation (ChIP) assay was employed to assess binding of p65 to the *PD-L1* promoter in 293 T cells transduced with p38 for 24 h using a p65 or IgG antibody. The experiments were repeated three times. (K) Representative example and summary data (n = 5) quantifying the expression of CD107a and IFN- γ in NK cells following their incubation with K562 cells for 24 h and then with the anti-PD-L1 mAb AZ in the absence or presence of 1 μ M p38 inhibitor SB202190 or SB203580. Two paired groups were compared by paired t test. Paired t test (E, F and J) was used for two-group comparisons and one-way ANOVA with repeated measures for donor-matched 3 or more groups (C, D, I, and K). *P* values were adjusted by the Holm-Sidak method. *, *P* < 0.05; **, *P* < 0.01; ***, *P* < 0.001; ****, *P* < 0.0001; NS, not significant.